33RD CONGRESS
OF THE INTERNATIONAL COUNCIL
OF THE AERONAUTICAL SCIENCES
STOCKHOLM, SWEDEN, 4-9 SEPTEMBER, 2022

ICAS 2022 SWEDEN

INFLUENCE OF OVERALL LAYOUT DESIGN OF COMPOUND MULTI-ROTOR VEHICLES ON FLIGHT PERFORMANCE

Yuke Huang[1], Mai Bando[2] & Shinji Hokamoto[3]

[1] Department of Engineering, Kyushu University, Japan
[2] Department of Engineering, Kyushu University, Japan
[3] Department of Engineering, Kyushu University, Japan

Abstract

In the design of multi-rotor vehicles, it is very important to predesign the overall layout from the perspectives of fluid dynamics, flight dynamics, and control performance. However, there is currently no unified guiding principle. In addition, traditional multi-rotor vehicles are usually not capable of high-speed flight and long endurance. This study discusses a kind of compound multi-rotor vehicle configurations and analyze the influence of the overall layout of multi-rotors on flight performance by utilizing Blade Element Momentum Theory (BEMT) and Particle Swarm Optimization (PSO). First, the flight dynamics model of the compound multi-rotor aircraft is established based on BEMT. Next, by using the PSO algorithm, aiming at the longest cruising distance, some results of proper layouts are shown according to different rotor sizes, positions, wing area, propeller sizes and rotating speeds. Finally, according to the simulation results, the influence of each independent variable on the optimal layout is analyzed. The results show that the method proposed in this paper can be applied as a guideline for the layout design of multi-rotor vehicles, and the compound multi-rotor has better flight performance than the traditional multi-rotor.

Keywords: compound multi-rotor vehicle, particle swarm optimization, optimal layout design, blade element momentum theory, guiding principle.

1. General Introduction

In recent years, various types of multi-rotor vehicles have been designed and developed by advanced institutes and companies worldwide [1]. This research is supported by two backgrounds. On the one hand, small unmanned air vehicles (UAVs, frequently called 'drones') are becoming more and more popular all over the world. Usually, multi-rotor vehicles can accomplish complex tasks such as aerial photography, agriculture, disaster relief, aerial work, logistics and transportation with a relatively simple mechanism and controller. On the other hand, most of large multi-rotor aircraft for manned or cargo transportation use fossil fuel as energy, CO_2 emission becomes an issue of widespread concern. As shown in Figure 1, the forecast published by International Civil Aviation Organization in 2012 [2] predicted that CO_2 emission generated by aircrafts will become almost double that of 2022. Therefore, due to energy saving and emission reduction, electric vertical take-off and landing (eVTOL) aircrafts are expected to replace traditional jet aircrafts, as eVTOL aircrafts are expected to reduce not only CO_2 but also noise and maintenance cost. Moreover, they allow greater flexibility in the layout of rotors because the motors and batteries are smaller and lighter than traditional mechanical systems, and they can be distributed at separate positions. However, due to the lower energy density of lithium batteries than fossil fuel, current electric multi-rotors have very short flight endurance. In order to solve this problem, the overall layout of the multi-rotor should be optimized to improve the flight efficiency.

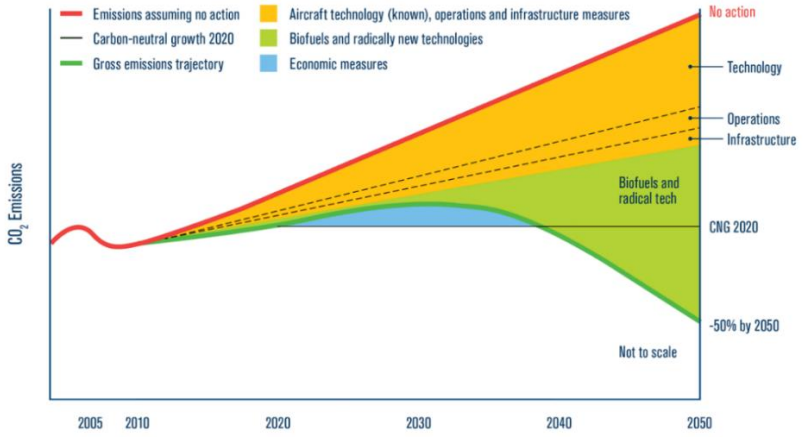

Figure 1 – Forecast of CO_2 emissions from aircraft by 2050.

Generally, in the design of multi-rotor vehicles, rotor number and layout have a significant influence on flight performance in terms of both fluid dynamics and aerodynamics. Companies around the world have designed a variety of layouts, however, there are currently no guidelines to determine these parameters. It should be noted that a proper design depends on different flight requirements (payload, cruise speed, flight altitude/distance, etc.), flight area (urban, mountain, or sea), and expected missions. Usually, the flight conditions for a small UAV are typically as follows: maximum speed of several tens of km/h, flight time less than one hour, and flight altitude less than several hundred meters. However, motorized airplanes, as alternatives to jet planes, are expected to fly at higher speeds over longer distances and carry several passengers. Therefore, the proper configuration of multi-rotor vehicles will naturally vary according to specific flight requirements, conditions or 'design philosophy'. This difference can be seen in the diversity of multi-rotors currently in development: Vahana [3] by Airbus, VoloCity [4] by Volocopter, Cora [5] by KittyHawk, Ehang 184 [6] by Ehang, etc. Moreover, N3-X [7] by NASA, as a future motorized airplane, has a notably different rotor layout compared with smaller UAVs.

Previous researches for eVTOL treat multi-rotors, fixed-wing, and tilt-rotors separately. At present, there are also many studies for compound multi-rotors such as shown in Figure 2, which have rotors for lift force, fixed-wing, and propellers for propulsion force. It is well known that multi-rotors vehicles can complete tasks such as vertical take-off and landing, and hovering in the air. Fixed-wing aircraft can fly at high speeds and have a large cruising range. This study discusses compound multi-rotor vehicle configurations and analyze the influence of the overall layout on flight performance. In previous research, the difference between the compound multi-rotor and tilt-rotor vehicles is believed as follows. The lift and thrust of the tilt-rotor vehicle are generated by common devices, which reduces the dead weight and has better aerodynamic characteristics and flight efficiency. In contrast, the compound multi-rotor vehicle has independent lift and thrust devices, which can avoid complex and unstable transition process of tilt-rotor vehicle. However, independent devices will also become dead weight and reduce flight performance. Therefore, this study proposes to add wings, propellers, etc. to the multi-rotors, a reasonable output ratio can be allocated by analyzing the different effects of each device on the flight performance, and the efficiency can be improved.

Figure 2 – Electric compound multi-rotor vehicle.

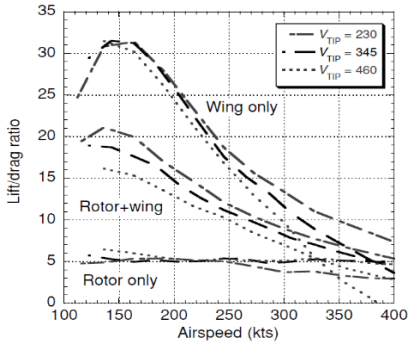

Figure 3 – Lift-to-drag ratio of rotor and wing.

1.1 Previous Researches

The research related to compound rotorcraft is very extensive, only a few are listed here. The early compound rotorcrafts were dominated by compound helicopters [8]. In the 21st century, the United States and Europe successively launched a series of compound helicopters and conducted test flight experiments [9]. Theoretical research on compound helicopters mainly focuses on overall parameter design, manipulation characteristics, aerodynamic characteristics under high advance ratio, as well as aerodynamic disturbances. Orchard and Newman [10] studied the overall configuration of the compound helicopter, in which the wing adopts a medium-thickness high-lift airfoil, the aspect ratio is 6, the rotor has good transonic characteristics, and the lift distribution between the wing and the rotor can be adjusted. Floros and Johson [11] used CAMRAD II software to analyze the effect of rotor and wing on required power and lift-to-drag ratio. The study pointed out that the combination of rotor and wing can significantly improve the lift-to-drag ratio, as shown in Figure 3. Low-speed rotors can reduce the required power of helicopter. When flying at a high speed, it is a better choice for the wings to bear most of the lift.

2. BEMT and Compound Multi-rotor Modelling

Blade element theory was proposed by Froude [12] and Drzewiecki [13] at the end of the 19th century. In 1926, Betz proposed Blade Element Momentum Theory (BEMT) to account for the sudden rotation of the flow by actuator disk [14]. Since then, correction methods for wingtip stalls and blade-root loss have been continuously proposed based on BEMT [15].

BEMT is a combination of blade element theory and momentum theory. According to the forces on small blade elements, the thrust and power of a rotor can be obtained by integrating the micro-elements into the entire blade [16].

The flight performance indicators of multi-rotors usually include ceiling altitude, flight speed, maximum rate of climb, flight range, flight time, etc. And the basis for discussing these indicators is to obtain the required power of the multi-rotor. There are generally two methods for calculating required power: basic analysis and trim analysis. The basic analysis method uses BEMT or the Pitt-Peters dynamic inflow model to analyze the force of the blade, and obtain the induced velocity distribution on the rotor plane, so as to obtain the required power, including the induced power, the profile power, the parasite power, etc. In the trim analysis, the derivative of each state variable is set to zero, and the trim solution for stable flight can be obtained. Then, calculate the aerodynamic force and torque, and obtain required power.

2.1 Momentum Theory

According to momentum theory, the value of the momentum change of the fluid flowing through the rotor plane in unit time is equal to the force acting on the fluid by the rotor. Then, according to the definition of power, the rotor thrust and power can be expressed as follows:

$$T = 2\rho V_1 S_1 v_1 = 2\rho\pi R^2 \left(V_0 + v_1\right) v_1 \tag{1}$$

$$P = 2\rho\pi R^2 \left(V_0 + v_1\right)^2 v_1 \tag{2}$$

where ρ is the air density, and S_1 is the rotor area with radius R. V_1 and v_1 are air velocity and induced velocity at rotor plane, respectively. Actually, each velocity in the equations is often expressed in dimensionless form according to the wingtip velocity ωR such as $\bar{V}_0 = V_0/\omega R$. Similarly, the thrust T and power P can be expressed in dimensionless form as $\rho\pi R^2 \left(\omega R\right)^2$ and $\rho\pi R^2 \left(\omega R\right)^3$, respectively. Then, the dimensionless expressions of the thrust and power coefficients are obtained as

$$C_{\mathrm{T}} = \frac{T}{\rho\pi R^2 \left(\omega R\right)^2} = 2\left(\bar{V}_0 + \bar{v}_1\right)\bar{v}_1 \tag{3}$$

$$C_{\mathrm{P}} = \frac{P}{\rho\pi R^2 \left(\omega R\right)^3} = 2\left(\bar{V}_0 + \bar{v}_1\right)^2 \bar{v}_1 \tag{4}$$

The rotor can be divided into infinite concentric rings along the radial direction of the blade, where

the thrust of each ring is expressed as

$$\mathrm{d}T = 2\rho\left(V_0 + v_1\right)v_1\mathrm{d}A \tag{5}$$

Here, dA ($=2\pi r\mathrm{d}r$) is the area of the concentric rings. Finally, the differential form of the thrust coefficient can be expressed as follows [17]:

$$\mathrm{d}C_\mathrm{T} = \frac{\mathrm{d}T}{\rho\pi R^2\left(\omega R\right)^2} = \frac{2\rho\left(V_0 + v_1\right)v_1\mathrm{d}A}{\rho\pi R^2\left(\omega R\right)^2} = 4\left(\bar{V}_0 + \bar{v}_1\right)\bar{v}_1\bar{r}\mathrm{d}\bar{r} \tag{6}$$

where $\bar{r} = r/R$ is the dimensionless radius of the blade.

2.2 Blade Element Theory

The essence of blade element theory is to divide a blade into infinitely small elements and establish a coordinate system to obtain expressions for force and power.

Figure 4 shows a schematic diagram of a blade rotating around a vertical axis. In this figure, u_T, u_P and u_R are the horizontal, vertical, and radial air inflow velocity components, respectively. θ, α and φ indicate the blade angle, angle of attack, and air inflow angle, respectively. It should be noted that the influence of its velocity component u_R in the radial direction is neglected for simplicity (that is, the drift effect of the blade is omitted) [18].

For the blade number *N*, the thrust and power of a blade element can be expressed by the lift *d*L and drag *d*D as

$$\mathrm{d}T = N\mathrm{d}z = N\left(\mathrm{d}L\cos\phi - \mathrm{d}D\sin\phi\right) \tag{7}$$

$$\mathrm{d}P = N\mathrm{d}x\cdot\omega r = N\left(\mathrm{d}L\sin\phi + \mathrm{d}D\cos\phi\right)\omega r \tag{8}$$

Here, 'solidity' [19] is often defined as the ratio of the area of the blade to the area of the paddle as

$$\sigma = \frac{NcR}{\pi R^2} = \frac{Nc}{\pi R} \tag{9}$$

where *c* is the chord length of the blade [20]. Then, differential expressions for the thrust and power coefficients can be given as [21]

$$\mathrm{d}C_\mathrm{T} = \frac{1}{2}\sigma C_\mathrm{L}\bar{r}^2\mathrm{d}\bar{r} \tag{10}$$

$$\mathrm{d}C_\mathrm{P} = \frac{1}{2}\sigma\left(\phi C_\mathrm{L} + C_\mathrm{D}\right)\bar{r}^3\mathrm{d}\bar{r} \tag{11}$$

where C_L and C_D are the lift and drag coefficients, respectively.

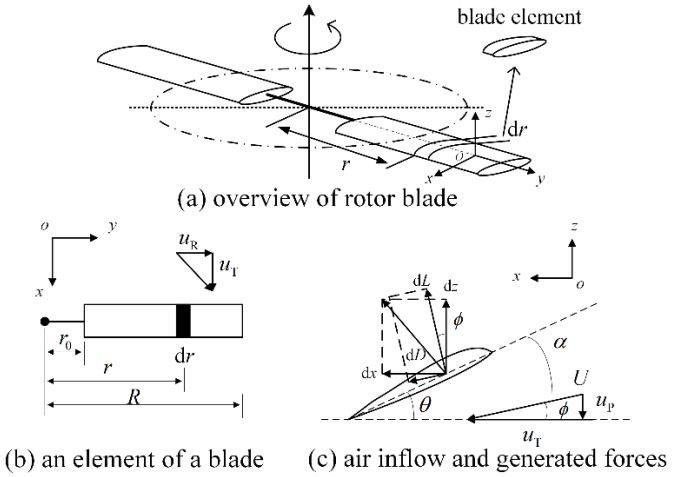

Figure 4 – Diagram of blade element theory.

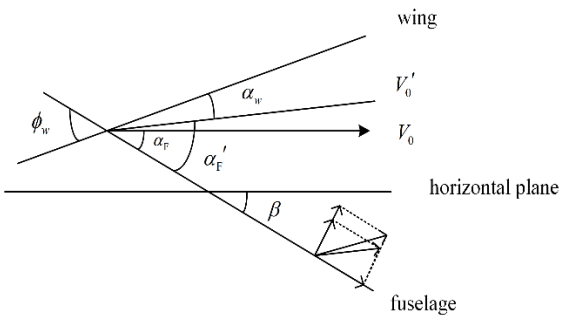

Figure 5 – Diagram of wing modelling.

2.3 Rotor Module

For the compound multi-rotors proposed in this paper, the power system is mainly divided into three parts: rotor system, wing system and propeller system. Using the BEMT described above, the rotor

system is first analyzed.

Considering that the forward tilt angle of the aircraft body is β, trigonometric functions are approximated at small angles, and infinitesimal quantities above the second order are ignored. Combining Equations (6) and (10), the following results can be obtained:

$$4\lambda\left(\lambda-\lambda_0\sin\beta\right)\bar{r}=\frac{1}{2}\sigma\bar{r}^2C_{\mathrm{L}}=\frac{1}{2}\sigma a\left(\theta\bar{r}^2-\lambda\bar{r}\right) \tag{12}$$

where, λ is the inflow ratio, referring to the ratio of the air inflow velocity to the wingtip rotational linear velocity. λ_0 is the inflow ratio of the forward speed. a describes how the lift coefficient changes according to the angle of attack. By solving Equation (12), λ can be obtained in terms of $\bar{r}$ as follows:

$$\lambda\left(\bar{r}\right)=\sqrt{\left(\frac{\sigma a}{16}-\frac{\lambda_0\sin\beta}{2}\right)^2+\frac{\sigma a}{8}\theta\bar{r}}-\left(\frac{\sigma a}{16}-\frac{\lambda_0\sin\beta}{2}\right) \tag{13}$$

After solving for λ, C_{T} and C_{P} can be integrated through Equations (10) and (11), so that T and P can be obtained by using Equations (3) and (4), respectively.

2.4 Wing Module

Figure 5 shows the diagram of wing modelling. The tilt angle of the fuselage to the forward direction (horizontal plane) is β. The angle between the wing and the fuselage is ϕ_w. Since the aircraft has a forward speed V_0, the velocity can be decomposed into the body axis system as follows:

$$\begin{cases} V_{wx}=V_0\cos\alpha_{\mathrm{F}} \\ V_{wy}=0 \\ V_{wz}=V_0\sin\alpha_{\mathrm{F}}+\varepsilon v_i \end{cases} \tag{14}$$

where, α_{F} is angle of attack of fuselage. Actually, due to the aerodynamic interference between wing and rotor, the induced velocity v_i produced by the rotor has an effect on the airflow over the wing. ε is the interference coefficient, which is taken as 0.8 in this paper. Therefore, the actual angle of attack of fuselage under interference is

$$\alpha_{\mathrm{F}}{}'=\arctan\frac{V_{wz}}{V_{wx}} \tag{15}$$

The lift and drag generated by the wing can be obtained.

$$\begin{cases} L_w=q_wS_wC_{\mathrm{L}w} \\ D_w=q_wS_wC_{\mathrm{D}w} \end{cases} \tag{16}$$

where q_w is the dynamic pressure. S_w, $C_{\mathrm{L}w}$ and $C_{\mathrm{D}w}$ are wing area, lift coefficient and drag coefficient, respectively. Finally, the lift and drag along the flight direction can be obtained.

$$\begin{cases} L_w^B=L_w\cos\left(\alpha_{\mathrm{F}}{}'-\beta\right)-D_w\sin\left(\alpha_{\mathrm{F}}{}'-\beta\right) \\ D_w^B=L_w\sin\left(\alpha_{\mathrm{F}}{}'-\beta\right)+D_w\cos\left(\alpha_{\mathrm{F}}{}'-\beta\right) \end{cases} \tag{17}$$

2.5 Propeller Module

Similar to the rotor, the propeller is also modeled using BEMT. However the difficulty is that the propeller plane is perpendicular to the direction of air flow. At high speeds, the air inflow velocity may be close to or even larger than the blade linear velocity [22]. Therefore the data cannot be approximated like a rotor. Moreover, at high speed, if the propeller rotation speed is not enough, it is easy to generate negative angle of attack and negative lift. This situation is prone to occur near the root of the blade. In the actual design, part of the propeller root can be cut off to avoid this situation.

The lift coefficient of the propeller is expressed as

$$\mathrm{d}C_{\mathrm{T}} = \frac{1}{2}\sigma\bar{U}^2\left(C_{\mathrm{L}}\cos\phi - C_{\mathrm{D}}\sin\phi\right)\mathrm{d}\bar{r} \tag{18}$$

where $\bar{U}$ is the air velocity of the propeller and can be expressed as

$$\bar{U}^2 = \frac{V_1^2 + (\Omega r)^2}{(\Omega R)^2} = \lambda^2 + \bar{r}^2 \tag{19}$$

After calculation and arrangement, the following equation can be obtained

$$4\lambda(\lambda - \lambda_0)\bar{r} = \frac{1}{2}\sigma\left(\lambda^2 + \bar{r}^2\right)\left(C_{\mathrm{L}}\cos\phi - C_{\mathrm{D}}\sin\phi\right) \tag{20}$$

In the actual calculation, since λ is obtained according to the integral of blade element, the parameter expression in matrix form can be obtained by the method of numerical integration. Then use the computer to find the numerical solution of the unknown parameter in the expression.

3. PSO Algorithm

Particle Swarm Optimization (PSO) is an evolutionary computation algorithm proposed in 1995 [23]. In the algorithm, starting from random positions, a population of candidates (called particles) moves in a search space to find better positions through an iterative process.

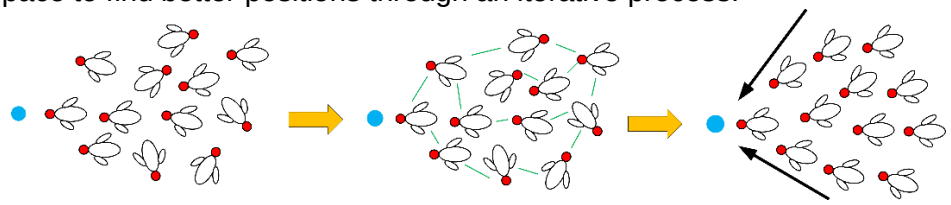

Figure 6 – Schematic diagram of PSO principle.

As shown in Figure 6, PSO was originally developed based on the predation behavior of birds. When a bird discovers food, it shares the location with other birds through information transmission, thereby gradually bringing the entire flock of birds to the food. The basic idea of PSO is to share personal information to all so that the whole can converge towards a goal from disorder to order.

PSO is initialized as a group of particles, and at each iteration, the particles update their positions by tracking two values: the individual optimal value, expressed by ‘pbest’, and the global optimal value, expressed by ‘gbest’. Specifically, the motion of each particle is expressed by the following two equations to update its position and velocity:

$$x_i(t+1) = x_i(t) + v_i(t+1) \tag{21}$$

$$v_i(t+1) = w\cdot v_i(t) + c_1\cdot\mathrm{random}\cdot\left(x_i^{pbest} - x_i(t)\right) + c_2\cdot\mathrm{random}\cdot\left(x_i^{gbest} - x_i(t)\right) \tag{22}$$

where x and v are the particle position and velocity (c_1, c_2 are design parameters). The parameter w is called the inertial factor; as w increases, the global search ability becomes stronger, but the local search ability becomes weaker.

Frequently, to obtain better optimized results by balancing both global and local search abilities, the following linearly decreasing weight (LDW) is used:

$$w^t = \frac{(w_{ini} - w_{end})(t_f - t)}{t_f} + w_{end} \tag{23}$$

where w_{ini} and w_{end} are the initial and final inertia factors, respectively, and t_f represents the maximum number of iterations.

4. MATLAB Simulation and Results

As described above, PSO utilizes ‘swarm intelligence’ to find better solutions in a multi-variable space. Furthermore, it can deal with multiple constraints by using penalty functions in its evolutionary process. In the practical design of multi-rotor vehicles, the objective function and constraints in the PSO process strongly depend on the mission purposes and flight conditions/environments of the vehicles. Thus, as an example, this study considered the max cruising distance of a vehicle as the objective function.

4.1 Specific Conditions of Layout Design

In the actual design of compound multi-rotors, many parameters should be considered. In this study, the layout design is performed under the following simplified conditions. All rotors are assumed to be on a plane and not overlap each other nor the fuselage of the vehicle. All rotor sizes are assumed to be the same so that the optimal results can be found by the PSO algorithm in the two-dimensional plane. Moreover, as the vehicle can move equally in four quadrants, the rotors are supposed to be symmetrically placed in each quadrant of the rotor-plane. Considering a 1-2 passenger vehicle, payload *M* is set as 200 kg. Furthermore, because the blade specifications affect the rotor's thrust and power, the blade number is set as four, and the blade's pitch angle is assumed 0 degree at its wingtip and linearly changes by 17 degrees at the root. Besides, a rotor's maximum size is limited to 3 m. Wings are regarded as rectangular, and have two propellers of the same size.

The other parameters to specify the rotor's thrust and power are set as follows. The air density is assumed to $\rho = 1.225$ kg/m^3, under a standard atmosphere of 1 atm at $15\,°C$. The battery's energy density is set as $\rho_e = 0.20$ kWh/kg based on lithium ion battery data [24]. Referring to other multi-rotors, the wing and rotor aspect ratios are set to 6 and 10, respectively. The motor's power-weight ratio is set to $\rho_p = 6.0$ kW/kg based on the current state-of-the-art [25]. For the arms to support the rotors, aluminium is a widely used material, and its cross-section is assumed to be a hollow circular shaft with 20% the thickness of the radius. Table 1 summarizes the specifications explained above.

Table 1 PSO parameter settings for design process

Parameter	Value
Airframe mass including payload $M\,[\mathrm{kg}]$	200
Battery mass $m_{\mathrm{e}}\,[\mathrm{kg}]$	200
Battery energy density $\rho_{\mathrm{e}}\,[\mathrm{kWh/kg}]$	0.20
Number of rotors *n*	4
Blade aspect ratio AR_r	10
Wing aspect ratio AR_w	6
Motor thrust-to-weight ratio $\rho_{\mathrm{p}}\,[\mathrm{kW/kg}]$	6.0
Rotor diameter limit $D_r\,[\mathrm{m}]$	1-3
Wing span limit $D_w\,[\mathrm{m}]$	1-3
Propeller diameter limit $D_p\,[\mathrm{m}]$	0.5-3
Arm material	Aluminium
Blade angle at blade-root $\theta[°]$	17
Blade number *N*	4

4.2 PSO Program Process

In this study MATLAB software is utilized to write the PSO optimization algorithm program to realize the design of the optimal layout of the compound rotor. The specific process is shown in Figure 7.

First the numbers of particles and iterations are set, which can be properly determined by the method of [26]. The initialization of particles includes random setting of initial positions, initial parameters and the range of constraint functions. Next the thrust coefficient and power coefficient of rotor system, wing system and propeller system are calculated by each module, respectively. Then a series of thrust and power which are dependent on rotating speeds are determined one by one. It is worth noting that each set of thrust data must meet: The sum of rotor lift and wing lift must be greater than gravity, and the sum of rotor thrust and propeller thrust must be greater than drag. Under these conditions the total power *P* of the multi-rotor is obtained, which is regarded as cruising power. Finally, the maximum cruising distance is obtained through the objective function.

The above is the process of one iteration of one particle. Update the position parameters and velocity parameters of each particle through the equations shown in the figure, and return to the parameter module for multiple iterative calculations, so that to the optimal layout can be found.

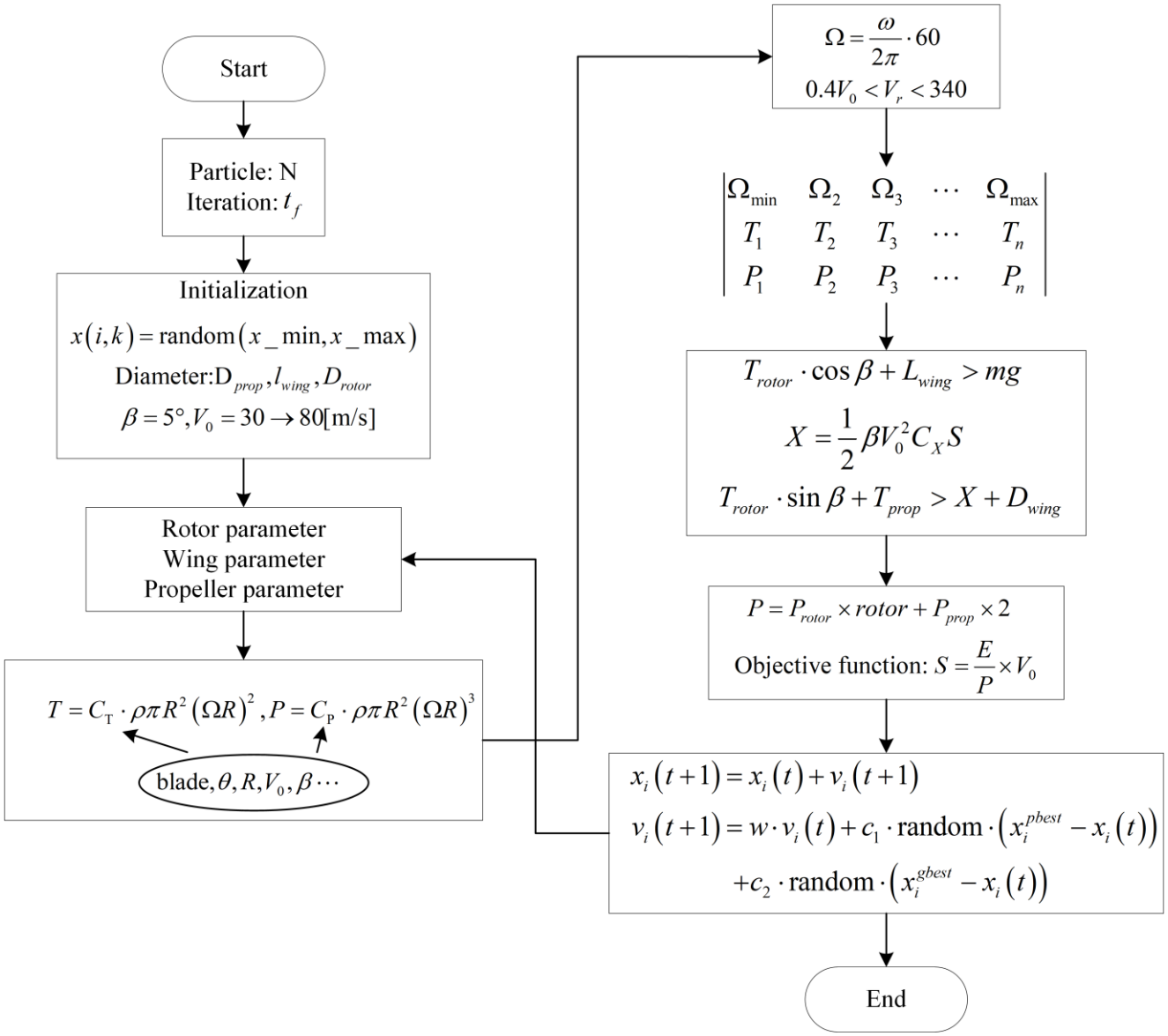

Figure 7 –The process of optimal layout design by PSO.

4.3 Simulation Results

This section analyzes the simulation results. The first is the simulation results obtained according to the PSO optimization algorithm. Here, four calculations are taken as an example.

Figure 8 shows the typical preferable layout obtained by PSO. For simplicity, this study only analyzes the case of 4 rotors. The case of 6, 8 or more rotors is not discussed here. Due to the symmetry, only a quarter of the multi-rotors, that is, the first quadrant portion, is shown in Figure 8. The longitudinal axis direction is the forward direction of the multi-rotor. The axes in the figure represent lengths [m]. The black circles are the rotors, the blue at the origin indicates a quarter of the cabin, and the red line is the arm to support the rotors. Furthermore, the orange rectangles represent the wings. There are two propellers, which are fixed to the wings and pointed forward. From the front view of the aircraft, the green circles represent the propellers. At the bottom of the figure, *S* represents the optimal result obtained from the simulation, that is, the maximum cruising distance [km], and V_0 represents the required flight speed [m/s].

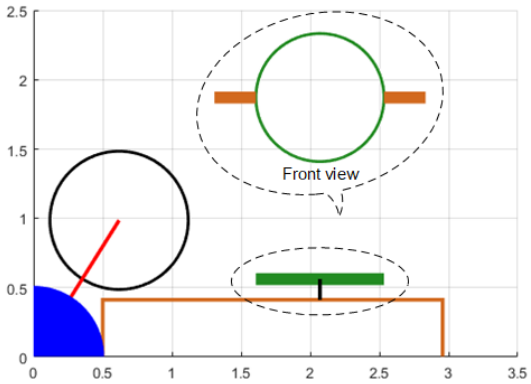

(a) $S=125.0591, V_0=60$

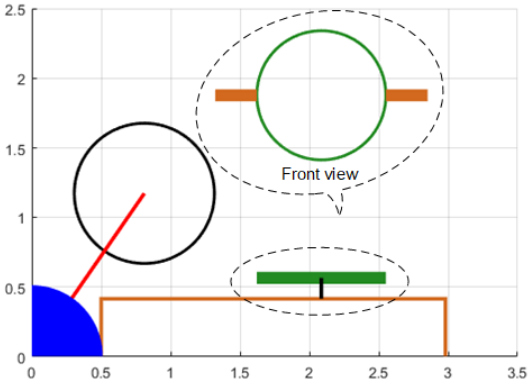

(b) $S=123.1065, V_0=60$

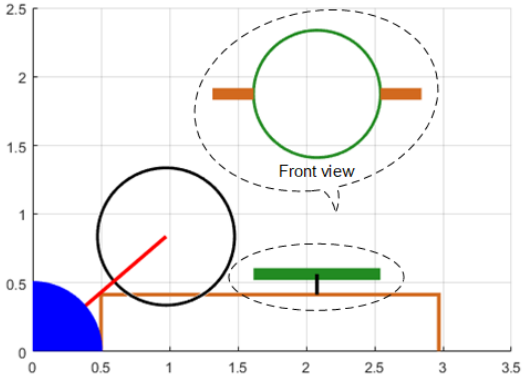

(c) $S=124.0865, V_0=60$

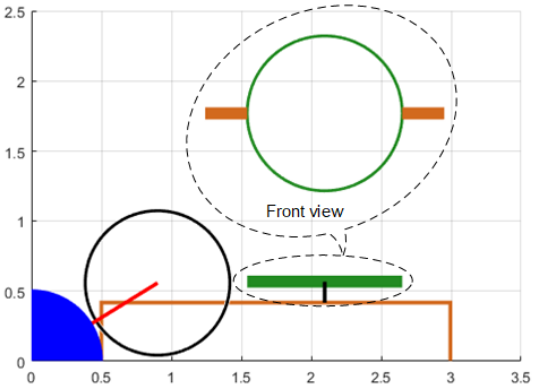

(d) $S=123.4014, V_0=60$

Figure 8 – Simulation results of optimal layout of compound multi-rotors.

It can be seen from Figure 8 that the results of the optimal layout of the compound multi-rotor vehicles are basically similar, which indicates the proposed calculation method according to PSO in this study is stable, and the calculation results can converge well. For simplicity, this study regards the fuselage as a simple sphere. The shape can be adjusted based on factors such as the flight mission/environment.

The results of multiple simulations show that the maximum cruising distance is about 124 km. And the flight speed is set to vary between 30–80 m/s, but the optimal result is 60 m/s, indicating that the flight speed also affects the optimal layout, and flying at a speed of 60 m/s can achieve the maximum cruising distance. It is worth noting that the diameter ranges of the rotor and propeller are set to 0.5-3 m and 1-3 m, respectively. The wingspan range is set to 1-3 m. In the actual calculation, the rotor diameter could have been smaller, but considering that the rotor needs enough lift to take off (about 450-500 kg) during the vertical take-off and landing phase, a minimum value should be set. The figure shows that the propeller needs to be of sufficient size in order to maintain sufficient thrust at high speeds. The rotor diameter should be as close to the lower limit as possible, and the wingspan should be as large as possible to ensure sufficient lift. This tendency indicates that the lift efficiency (or lift-to-drag ratio) of a wing is higher than that of a rotor at high speed.

In addition, it is observed that the length of the arm connecting the rotor and the body changes irregularly. In previous research [26], taking the minimum take-off weight as the objective function, the mass of the arm had a great influence on the optimal layout result. Therefore, the arm was as close to the body as possible. However, in this study, the arm mass is only a small part. The most important reason is that in the current algorithm, in order to ensure the calculation efficiency, the growth gradient of the rotor and propeller rotating speed is relatively large. Consequently, it is not sensitive to the quality increment caused by the arm. This will be further optimized in subsequent

studies.

In order to analyze the results more intuitively, some simulation data are given in Table 2.

Table 2 PSO optimal layout simulation data

$S=125.0591, V_0=60$					
Position x	Position y	Propeller diameter		Wingspan	Rotor diameter
0.6183	0.9846	0.9261		2.4574	1.0000
Rotor lift	Rotor speed	Wing lift	Wing drag	Propeller thrust	Propeller speed
31.1	1909.9	2908.1	365.3	470.1	4525.7
$S=123.1065, V_0=60$					
Position x	Position y	Propeller diameter		Wingspan	Rotor diameter
0.8109	1.1726	0.9302		2.4803	1.0096
Rotor lift	Rotor speed	Wing lift	Wing drag	Propeller thrust	Propeller speed
31.7	1891.6	2962.7	372.2	477.4	4512.1
$S=124.0865, V_0=60$					
Position x	Position y	Propeller diameter		Wingspan	Rotor diameter
0.9752	0.8356	0.9282		2.4695	1.0019
Rotor lift	Rotor speed	Wing lift	Wing drag	Propeller thrust	Propeller speed
31.2	1906.3	2936.9	368.9	473.8	4518.8
$S=123.4014, V_0=60$					
Position x	Position y	Propeller diameter		Wingspan	Rotor diameter
0.9013	0.5564	1.1086		2.4945	1.0337
Rotor lift	Rotor speed	Wing lift	Wing drag	Propeller thrust	Propeller speed
33.2	1847.7	2996.7	376.4	481.1	3539.0

In Table 2, there are a total of four sets of data from top to bottom, corresponding to the four figures (a) (b) (c) (d) in Figure 8 respectively. In each set of data, position x and y represent the coordinates of the center of the rotor, followed by propeller diameter, wing span and rotor diameter. These five data are the parameters that need to be iteratively optimized in PSO. It can be indicated from the table that the positions, diameter and wingspan data are almost identical among the results obtained from the four sets of samples. Furthermore, as previously analyzed, the propeller diameter cannot be too small, otherwise it will not provide enough thrust. But it can't be too large, otherwise it will increase the required power of the aircraft. Since the wing has higher efficiency than the rotor, increasing the wing can effectively improve the lift-drag ratio of the aircraft. So the wing area are relatively larger. Finally, it has been verified by experiments that the optimal rotor size under the current situation should be around 0.6m. However, the aircraft is not always cruising. In the vertical take-off and landing stage, due to the small flight speed, the wing cannot provide enough lift, and the rotor needs to bear almost all the lift at this time. Therefore, the rotor cannot be too small, and the minimum size is set to 1m here, so the optimization result is close to the minimum value.

The following 6 data are respectively the rotor lift, rotating speed, the wing lift, drag, the propeller lift and rotating speed when cruising flight under this condition. It can be seen intuitively that the result of the program optimization is that when flying at high speed, the wing bears most of the lift, and the rotor only provides a very small part of the lift and forward thrust. In addition, the propeller bears almost all forward thrust, which is used to balance the drag of various parts such as the fuselage and wings. At this time, the compound multi-rotor is more inclined to the fixed-wing flight mode.

Moreover, note that in all optimization results, the flight speed is 60 m/s. Suppose that the flight speed becomes less than 60, the required power of the propeller will also decrease, and the flight time of the aircraft will increase as a result. However, the reduced speed multiplied by the increased time does not necessarily result in greater cruising distance. The same problem can also occur with increased flight speed, and more importantly, as mentioned in the propeller module, too fast flight

speed will cause the propeller to generate negative angle of attack and negative lift, which will seriously affect the thrust efficiency of the propeller.

The above is the proposed method and process of the optimal layout of the compound multi-rotor with PSO in this study, and several results have been obtained. However, it is also necessary to verify whether the results in Figure 8 and the data in Table 2 are really the optimal results.

The verification method used in this study is as follows: change the value of a variable in a small range while keeping other layouts basically unchanged, then calculate the cruising distance. The simulation results are as follows.

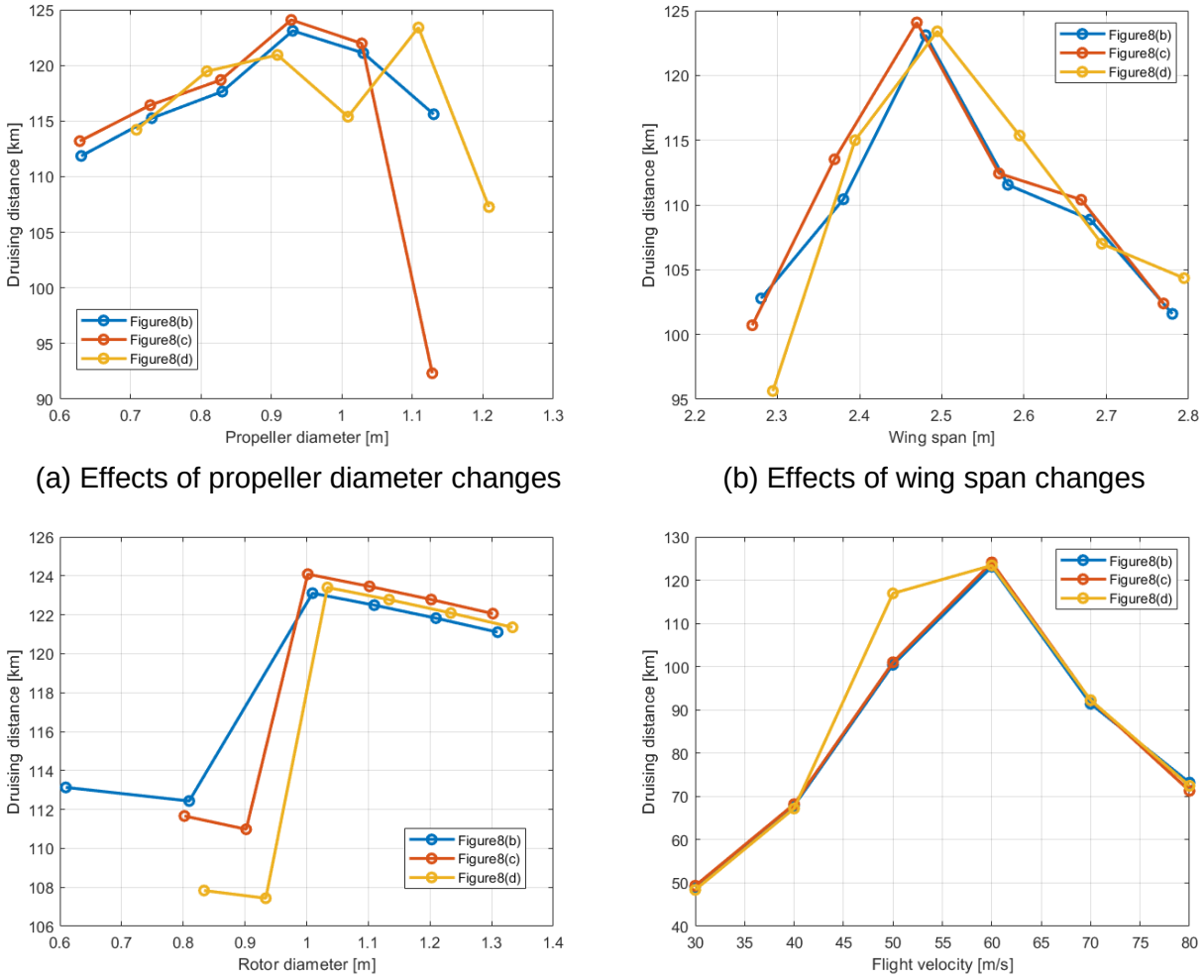

(a) Effects of propeller diameter changes

(b) Effects of wing span changes

(c) Effects of rotor diameter changes

(d) Effects of flight velocity changes

Figure 9 – Effects of layout parameter changes on optimal results.

In Figure 9, (a) (b) (c) (d) respectively represent the influence of the changes of propeller diameter, wing span, rotor diameter and flight speed on the optimal layout. There are three broken lines in each figure, respectively from the three sets of data (b) (c) (d) in Figure 8. The horizontal axis represents the variation range of each parameter, and the vertical axis represents the maximum cruising distance. From Figure 9, the following conclusions can be drawn:

The highest point of the data in each figure, that is, the maximum cruising distance, is consistent with the data obtained above. The trend of each line is basically the same. In other words, the proposed optimal layout design method of the compound multi-rotor with PSO is basically reasonable. The obtained results can indeed make the objective function achieve the maximum value, and in a small range, other layouts are not better than the obtained results.

Comparing Figure 9 (a) (b) (c) with (d), it can be found that the flight speed has the greatest impact on the cruising distance, this is due to the gradient setting of this study. When making changes to diameter and wingspan, the accuracy is 0.1 m, and the accuracy of flight speed changes is 10 m/s. So the changes brought by speed are more drastic.

Furthermore, combining the four graphs in Figure 9, it can be concluded that for the compound multi-

rotor with the conditions shown in Table 1, the optimal layout design should be: Four rotors with a diameter of about 1m. The diameter of 1m may not be the optimal value in the cruising state, but considering the lift in the vertical take-off and landing stage, the rotor should not be too small. Therefore, the rotor size range can be adjusted according to the actual task environment. However, since the lift efficiency of the wing is better than that of the rotor, the rotor tends to be as small as possible, and the aircraft tends to the fixed-wing flight mode. The unilateral wingspan is about 2.5m. In fact, in the case of ensuring sufficient lift, the wing also tends to be as small as possible. The diameter of the propeller is about 0.9m to 1m. The propeller is the most important thrust system and the most complex module. Too small cannot provide enough thrust, and too large will increase the required power. The design also needs to consider the problem of negative angle of attack. The flight speed is better around 60 m/s.

5. Conclusion

The overall layout design of multi-rotor vehicles has great influence on flight performance. In the practical multi-rotor vehicle design, the component size and layout are relatively decisive parameters for the flight performance. In this study, a design method of compound multi-rotor is proposed, PSO was utilized in the predesign for optimal layout design of compound rotors. First the compound rotor is modeled by BEMT. Then the PSO optimization algorithm is used to find the optimal layout. Finally, it is verified that the result obtained is indeed the optimal layout. Research data show that the proposed method can be applied as a guideline for the layout design of compound multi-rotor vehicles.

6. Future Work

This study only discusses the case where the number of rotors is 4 and the number of propellers is 2. According to different environments and missions, the optimal layout for different rotor numbers (6, 8, 10, or more) can be discussed.

This study does not consider the influence of weight on the optimal layout in detail. In actual design, weight will affect the required power of the aircraft. Therefore, from the reference [26], the rotor size can be analyzed firstly to meet the weight, and then the layout of other components can be analyzed.

This study is only for the speed range 30-60 m/s. Since the research object is urban manned aircraft, the range of lower speed (10+ m/s) or higher speed (100+ m/s) should be considered in the future.

7. Contact Author Email Address

The contact author email address: huang.yuke.020@s.kyushu-u.ac.jp

8. Copyright Statement

References

[1] Kim H, Lim D and Yee K. Development of a comprehensive analysis and optimized design framework for the multirotor UAV. *31st Congress of the International Council of the Aeronautical Sciences*, 9–14 September, Belo Horizonte, Brazil, 2018.

[2] ICAO (2016), ICAO Long-Term Traffic Forecasts.

[3] Airbus (2020) Acubed - We are the Silicon Valley innovation center of Airbus. Available at: https://acubed.airbus.com/ (Accessed 15 September 2020).

[4] Volocopter, (2020) VoloCity – the urban air taxi by Volocopter. Available at: https://www.volocopter.com/solutions/volocity/ (Accessed 16 September 2020).

[5] Kittyhawk (2020) Kitty Hawk. Available at: https://kittyhawk.aero/ (Accessed 3 September 2020).

[6] Ehang (2020) EHang | UAM - Passenger Autonomous Aerial Vehicle (AAV). Available at: https://www.ehang.com/ehang184/specs/ (Accessed 16 September 2020).

[7] NASA (2020) NASA. Available at: https://www.nasa.gov/ (Accessed 5 May 2020).

[8] Li J. Analysis on Technology Development of Compound Helicopter. *Journal of Nanjing University of Aeronautics and Astronautics*, Vol. 48, No.2, pp 149-158, 2016.

[9] Walsh D, Weiner S, Arifian K, et al. High Airspeed Testing of the Sikorsky X2 Technology Demonstrator. *67th Annual Forum Proceedings of the American Helicopter Society*, Virginia Beach, VA, 2011.

[10] Orchard M, Newman S. The Fundamental Configuration and Design of the Compound Helicopter. *Journal of Aerospace Engineering*, Vol. 217, No. 1, pp 297~315, 2003.

[11] Floros M W, Johnosn W. Stability and Control Analysis of the Slowed-Rotor Compound Helicopter. *Journal of the American Helicopter Society*, Vol. 52, No. 3, pp 239-253, 2007.

[12] Froude W. On the elementary relation between pitch, slip and propulsive efficiency. *Transactions of the Institute of Naval Architects*, Vol. 19, No.1, pp 47–65, 1878.

[13] Drzewiecki S. Méthode pour la détermination des éléments mécaniques des propulseurs hélicoïdaux. *Bulletindel Association Technique Maritime 3 Session*, 1893.

[14] Betz A. Screw propellers with minimum energy loss. *Göttingen Reports*, 193-213, 1919.

[15] Xiaoqing W. Research on Modeling and Control Technology of Unmanned Helicopter. *Nanjing University of Aeronautics and Astronautics*, 2009.

[16] Winslow J, Hrishikeshavan V and Chopra I. Design methodology for small-scale unmanned quadrotors. *Journal of Aircraft*, Vol. 55, No. 3, pp 1062-1070, 2018.

[17] Ryoji T. Aerodynamic characteristics of NACA4402 in low Reynolds number flows. *Journal of The Japan Society for Aeronautical and Space Sciences*, Vol. 54, No.631, pp 367–373, 2006.

[18] Ruopeng B, Binghe Z, Jianyong Z and Miao H. Influence of Pitch Angle on Aerodynamic Characteristics of Propeller. *Journal of Drainage and Irrigation Machinery Engineering*, Vol. 37, No. 4, pp 336–340, 2019.

[19] Capello E, Guglieri G and Quagliotti F. A design configuration and optimization for a multi rotor UAV. *In NATO RTO Symp. Intelligent Uninhabited Vehicle Guidance Systems*, 2009.

[20] Theys B, Dimitriadis G, Hendrick P and De Schutter J. Influence of propeller configuration on propulsion system efficiency of multi-rotor Unmanned Aerial Vehicles. *2016 International Conference on Unmanned Aircraft Systems*, 7–10 June, Arlington, VA, USA, 2016.

[21] Huirong J, Zhicheng D, Ming Z and Xueshou P. On Modeling and Control of Quadrotor Aircraft with Variable Blade Pitch. *Electronics Optics and Control*, Vol. 22, No. 10, pp 48–55, 2015.

[22] Dong C. Research on Fight Performance of a Conventional Configuration Compound Helicopter. *Nanjing University of Aeronautics and Astronautics*, 2018.

[23] Kennedy J and Eberhart R. Particle Swarm Optimization. *Proceedings of IEEE International Conference on Neural Networks*, IV, 1942–1948, 1995.

[24] Choi J. W. and Aurbach D. Promise and reality of post-lithium-ion batteries with high energy densities.

Nature Reviews Materials, Vol. 1, No. 4, pp 1-16, 2016.

[25]Siemens, (2020) Siemens. Available at: https://new.siemens.com/global/en.html (Accessed 12 July 2020).

[26]Huang Y, Watanabe T, Bando M and Hokamoto S. PSO algorithm parameter settings and optimal multi-rotor layout design. *International Journal of Sustainable Aviation*, Vol. 8, No. 2, pp 116-135, 2022.